# Journal of Materials Chemistry A

Accepted Manuscript


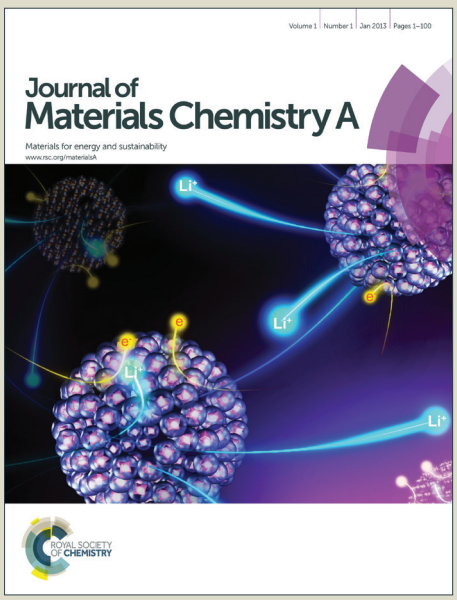





ROYAL SOCIETY OF CHEMISTRY

www.rsc.org/materialsA

Cite this: DOI: 10.1039/c0xx00000x

www.rsc.org/xxxxxx

ARTICLE TYPE

# CMK3/ Graphene-N-Co, a low-cost and high-performance catalytic system

Xiang-Jun Huang [a], Yi-Guo Tang [a], Long-Fei Yang [a], Ping Chen [a,*] Qing-Sheng Wu [b,*], Zhen Pan [a]

***Received (in XXX, XXX) Xth XXXXXXXXX 20XX, Accepted Xth XXXXXXXXX 20XX***
**DOI: 10.1039/b000000x**

**Abstract:** Excellent CMK3/graphene-N-Co (CMK3/G-N-Co) catalytic system was firstly prepared by a simple procedure. It shows excellent catalytic ability in the alkaline media for oxygen reduction reaction (ORR) and the half-peak potential is only 27 mV less than that of the commercial 20 % Pt/C catalyst. The product revealed superior stability and tolerance to methanol poisoning effects compared to the commercial 20 % Pt/C catalyst. The excellent performance is probably attributed to the doping of the nitrogen and cobalt elements in the CMK3/G, formation of a three-dimension nanoporous network structure by combining graphene with CMK3 and the promoted charge transfer across the carbon-Co interface and conductivity of the nanocomposite. Since the graphene oxide (GO) and CMK3 have become the commercially available materials, the CMK3/G-N-Co catalytic system for ORR is the promising alternatives to Pt in fuel cells practical application. The product may also have potential applications in the fields of metal-air batteries, lithium-ion batteries, supercapacitors, sensors and so on.

## 1. Introduction

Electrocatalysts for the oxygen reduction reaction (ORR) are crucial in fuel cells.[1-2] Because of the scarcity of platinum, developing non-precious metal or metal-free electrocatalysts for ORR with high activity remains a key issue.[3] Compared with traditional Pt-based catalysts, the non-precious metal or metal-free electrocatalysts possess strong durability and tolerance to methanol poisoning effects.[4-8] Though great progress has been made in the past several years, developing high-performance non-precious metal or metal-free electrocatalysts with cheap and commercially available materials is a great challenge in the practical application of fuel cell.[9-11]

Recently, heteroatom (N, B, S, P)-doped carbon electrocatalysts for ORR have been emerging as a promising metal-free electrocatalysts for ORR.[5] Especially, the N-doped carbon catalysts such as carbon nanotubes, graphene, nanofibers, carbon nanocage and carbon nanotube-graphene complexes have received increasing attention.[9,11-16] In addition, Fe or Co-doped carbon electrocatalysts for ORR have been found to exhibit excellent electrocatalytical performance.[17-20]

N-doped graphene has been a promising metal-free electrocatalysts for ORR, because of a large number of active sites and high conductivity. Recently, the graphene oxide (GO) can be manufactured on the large scale at low cost, which makes them potentially cost-effective and commercially available materials for practical application.[21-23]

The mesoporous carbon with pore size ranging from 2 to 50 nm can be a potential candidate electrocatalyst because of the high surface area, various pore sizes, and structures. So far, great progress in the preparation of mesoporous carbon material has been made.[24-25] As an ordered mesoporous carbon, CMK-3 can be manufactured on the large scale at low cost and has become the commercially available materials.[26-27]

Based on the above consideration and our recent study,[11,28, 29] here, CMK3/graphene-N-Co (CMK3/G-N-Co) catalytic system was firstly prepared by a simple procedure. The typical product shows excellent catalytic ability, stability and tolerance to methanol poisoning effects in the alkaline media for ORR. We develop a facile and readily scalable approach to synthesize the low-cost and high-performance electrocatalyst for the ORR.

## 2. Experimental section

### 2.1 Chemicals

CMK3 was purchased from Nanjing XFNANO Materials Tech Co., Ltd (Nanjing, China). Cobalt (II) acetate tetrahydrate was purchased from the Aladdin Reagent Co., Ltd. (Shanghai, China). Sulfuric acid ($H_2SO_4$, 98 %), potassium permanganate ($KMnO_4$, 99 %), hydrogen peroxide ($H_2O_2$, 30 %), sodium nitrate ($NaNO_3$) were purchased from Shanghai chemical reagent factory (Shanghai, China). All reagents are of analytical reagent grade and used without further purification.

GO was prepared by the exfoliation of natural graphite under acidic conditions according to the Hummer's method.[30] AFM image of the GO was shown in Figure S1 in the Supporting Information.

### 2.2 Preparation

**Preparation of CMK3/G-N-Co.** Scheme 1 showed the illustration of the proposed formation of the typical CMK3/G-N-Co catalytic system (2.4 wt% Co and 7.0 at% N). Firstly, 60.0 mg CMK3 was dispersed in the 10 mL distilled water and gradually added to the 30.0 mL GO solution (2.5 mg/ mL). Then, 13.0 mg cobalt (II) acetate tetrahydrate was gradually added to the mixture solution, which was stirred magnetically at 25 °C for 20 min. The dried mixture was obtained by freeze drying for 12 h. Finally, the dried mixture was annealed in $NH_3$ atmosphere at 950°C for 50 min and the product was obtained. CMK3/G-N-Co catalyst comprises the CMK3, graphene, nitrogen, and trace cobalt.

**Preparation of CMK3/G-N.** CMK3/G-N was made through the same steps as CMK3/G-N-Co without adding Co salt in the process.

**Preparation of CMK3-N-Co**. CMK3-N-Co was made through the same steps as CMK3/G-N-Co without adding GO in the process.

**Preparation of G-N-Co.** G-N-Co was made through the same steps as CMK3/G-N-Co without adding CMK3 in the process.

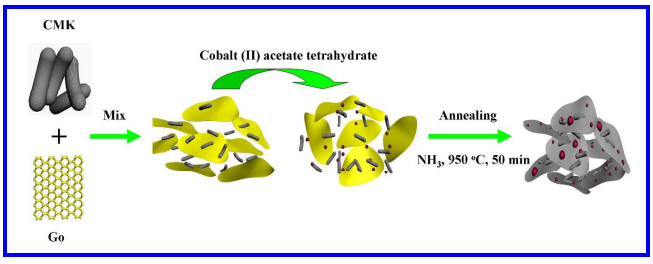


**Scheme 1.** Illustration of the proposed formation of the typical CMK3/G-N-Co.

### 2.3 Characterization

Scanning Transmission electron microscopy (STEM) images were recorded on a JEM-2100F with an EDX analytical system. STEM samples were prepared by drop-drying the samples from their ethanol suspensions onto copper grids. BET surface area was measured with a Micrometrics ASAP2020 analyzer (USA). X-ray photoelectron spectroscopic (XPS) measurements were performed on an X-ray photoelectron spectrometer (ESCALab MKII). Raman spectra were taken by an inVia-Reflex spectrometer (Renishaw). X-ray diffraction patterns (XRD) of the products were performed on an XD-3 X-ray diffractometer. The Co element contents in the catalysts were obtained from ICP (IRIS Intrepid II ICP-OES).

### 2.4 Electrochemical measurements

The electrochemical measurements were carried out in a three-electrode cell using CHI 852C electrochemical workstation (Shanghai Chenhua, China) at room temperature. Hg/HgO was used as reference electrode and platinum plate was used counter electrode. The ORR tests were carried out in $O_2$-saturated 0.1 M KOH solution at room temperature. In the **rotating disk electrode** (RDE) measurements, a glassy carbon (GC) disk with a diameter of 5 mm served as the substrate for the working electrode. For each sample, 10.0 mg of the sample was dispersed in the ethanol solution (5.0 mL) and ultrasonically for 30 min. Then, 10.0 μL of this suspension was dropped and adhered on the GC disk electrode using Nafion solution.[11, 28, 29] The working electrode was scanned at a rate of 20 $mVs^{-1}$ with the rotating speed from 400 rpm to 2000 rpm. In the **rotating ring-disk electrode** (RRDE) measurements, catalyst and electrode were prepared by the same method as above. Pt ring electrode was polarized at 100 mV (vs Hg/HgO) in $O_2$-saturated 0.1 M KOH solution.

## 3. Results and discussion

### 3.1 Electrocatalytical activities

The RDE results were shown in Figure 1. Figure 1a shows the RDE voltammograms in $O_2$-saturated 0.1 M KOH at room temperature (rotation speed 1600 rpm, sweep rate 20 $mVs^{-1}$). For the typical CMK3/G-N-Co, CMK3/G-N，CMK3-N-Co, G-N-Co and commercial 20 wt % platinum on carbon black (Pt/C) (Johnson Matthey Company), the value of half-peak potential was -138.0, -174.0, -156.0, -240.0 and -111.0, respectively. Compared to CMK3/G-N, CMK3-N-Co and G-N-Co, the CMK3/G-N-Co

shows the remarkably high half-peak potential and reduction current. The half-peak potential for the typical CMK3/G-N-Co is only 27 mV less than that of the commercial 20 % Pt/C catalyst. So far, though some non-precious metal or metal-free electrocatalysts for ORR have been reported, most of the catalysts still exhibit weak activity. Compared with these catalysts, the CMK3/G-N-Co shows the excellent catalytic ability in the alkaline media.[5, 11,13, 14, 15, 16]

RDE voltammograms for the typical CMK3/G-N-Co electrode at varying rotating speed (400-2000 rpm) were shown in the Figure 1b. Koutecky–Levich (K-L) plots were analyzed. The slopes of their best linear fit lines were used to calculate the number of electrons transferred ($n$) on the basis of the K-L equation:[13,28, 31]

$$\frac{1}{i} = \frac{1}{i_k} + \frac{1}{B \cdot \omega^{1/2}} \quad (1)$$

where $i$ is the measured current, $i_k$ is the kinetic current and $\omega$ is the electrode rotation rate. The theoretical value of the Levich slope ($B$) is evaluated from the following relationship:[13,28, 31]

$$B = 0.62 \cdot n \cdot F \cdot C_{O_2} \cdot D_{O_2}^{2/3} \cdot \nu^{-1/6} \quad (2)$$

$n$: the overall number of transferred electrons in the ORR process

$F$: the Faradaic constant (96485 C/ mol)

$C_{O2}$: the oxygen concentration (solubility) in 0.1 M KOH ($1.2\times10^{-6}$ mol cm$^{-3}$)

$D_{O2}$: the oxygen diffusion coefficient in 0.1 M KOH ($1.90\times10^{-5}$ cm$^2$ s$^{-1}$)

$\nu$ : the kinematic viscosity of the 0.1 M KOH (0.01 cm$^2$ s$^{-1}$).[32]

From the corresponding K-L plots ($i^{-1}$ vs. $\omega^{-1/2}$), it can be seen that the data exhibited good linearity and the number of electrons transferred (n) was estimated to be 3.4-3.9 at potentials ranging from -0.2 to -0.8 V (Figure S4, see the Supporting Information). Therefore, the typical CMK3/G-N-Co electrode reveals a four-electron pathway for ORR with much higher peak current and shows the remarkably enhanced electrochemical activities.

In the practical application, the catalyst for ORR should exhibit satisfactory tolerance to the fuel molecule, because it may pass across the membrane from the anode.[15,33] The typical CMK3/G-N-Co catalyst and Pt/C was exposed to 1.0 M methanol for testing possible poisoning effects, respectively. Figure 1c shows the RDE voltammograms in $O_2$-saturated 0.1 M KOH solution for the typical CMK3/G-N-Co and Pt/C with or without 1.0 M methanol. From the Figure 1c, compared to Pt/C, the typical CMK3/G-N-Co catalyst shows little activity loss, indicating excellent tolerance to methanol poisoning effects. The durability of the catalyst for ORR has been regarded as one of the most important issues.[8,31,34] Figure 1d shows the current-time (i-t) chronoamperometric response of the typical CMK3/G-N-Co and Pt/C electrodes. After 20000 seconds, the commercial Pt/C suffered from a 23.0 % decrease in current density while the typical CMK3/G-N-Co showed the 18.0 % loss of current density. The typical CMK3/G-N-Co revealed a better durability than the commercial Pt/C.

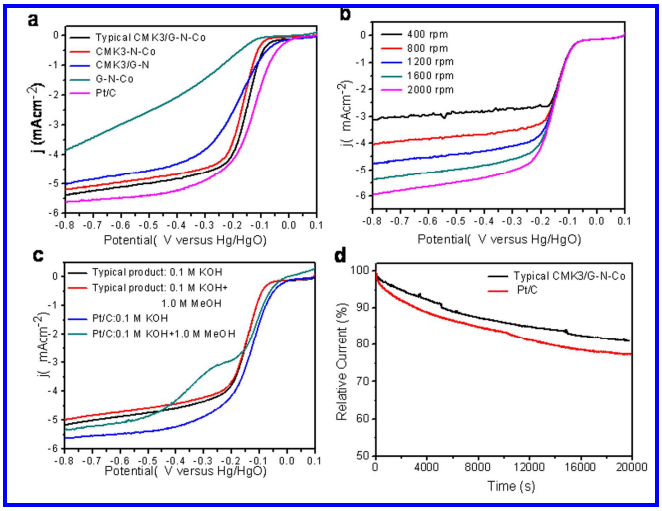


**Figure 1.** RDE results in alkaline media. (a) RDE voltammograms in $O_2$-saturated 0.1 M KOH at room temperature (rotation speed 1600 rpm, sweep rate 20 mV s$^{-1}$) for the typical CMK3/G-N-Co，CMK3/G-N，G-N-Co, CMK3-N-Co and Pt/C; (b) RDE voltammograms for the ORR at the typical CMK3/G-N-Co electrode at the various rotation speeds (sweep rate 20 mV s$^{-1}$); (c) RDE voltammograms in $O_2$-saturated 0.1 M KOH solution at room temperature (rotation speed 1600 rpm, sweep rate 20 mV s$^{-1}$) for the typical CMK3/G-N-Co and Pt/C with or without 1.0 M methanol; (d) Current-time (i-t) chronoamperometric response of the typical CMK3/G-N-Co and Pt/C electrodes at -0.65 V (vs Hg/HgO) in $O_2$-saturated 0.1 M KOH solution at a rotation rate of 800 rpm.

The selectivity of the four-electron reduction of oxygen for the typical catalyst was tested by RRDE technique. The $\%H_2O_2$ and the electron transfer number ($n$) were determined by the following equations:[9,31,35]

$$\%(H_2O_2) = 200 \times \frac{I_R / N}{I_D + I_R / N} \quad (3)$$

$$n = 4 \times \frac{I_D}{I_D + I_R / N} \quad (4)$$

where $I_D$, $I_R$ and N stands for the disk current, ring current and current collection efficiency of the Pt ring, respectively. The N was measured from the reduction of $K_3Fe[CN]_6$ according to the literature.[28,29,35] In

the experiment, the N is 0.35. Figure 2a shows the RRDE voltammograms in $O_2$-saturated 0.1 M KOH at room temperature (rotation speed 1600 rpm, sweep rate 20 $mVs^{-1}$) for the typical CMK3/G-N-Co, and Pt ring electrode was polarized at 100 mV (vs Hg/HgO) for detecting peroxide species formed at the disc electrode. The peroxide yield obtained from RRDE curves was shown in the Figure 2b. Surprisingly, the peroxide yield of typical catalyst remained below 6.0 % at the potentials from -0.8 to -0.1 V (vs Hg/HgO). The electron transfer number derived from the results of the RRDE test (Figure 2b) was calculated to be 3.8-3.9 from -0.8 to -0.1 V (vs Hg/HgO), revealing an intrinsic four-electron-transfer process.

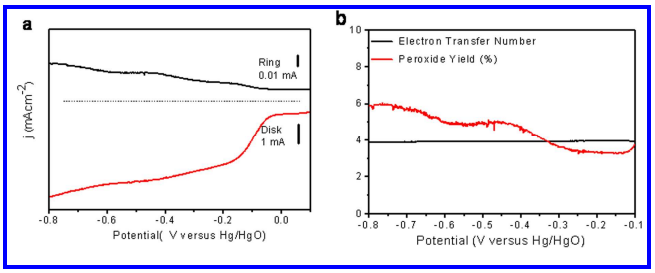


**Figure 2.** RRDE results for the typical CMK3/G-N-Co**.** (a) RRDE voltammograms for the ORR at the typical CMK3/G-N-Co in $O_2$-saturated 0.1 M KOH. The electrode rotation speed was 1600 rpm, sweep rate was 20 mV $s^{-1}$, and Pt ring electrode was polarized at 100 mV (vs Hg/HgO); (b) The electron transfer number (n) and peroxide yield obtained from RRDE curves.

According to the above results, the typical CMK3/G-N-Co shows excellent catalytic ability for ORR and the half-peak potential is only 27 mV less than that of the commercial 20 % Pt/C catalyst. The typical product revealed superior stability and tolerance to methanol poisoning effects compared to the commercial Pt/C.

### 3.2 Characterization

The scanning transmission electron microscopy (STEM, Figure 3a and b) clearly revealed the typical CMK3/G-N-Co nanocomposite including CMK3, graphene and cobalt nanoparticles with the size from 5 to 45 nm. The elemental mapping analysis (Figure 3c-f) suggested the presence of N, C, O, and Co components in the product. The N, C and O elements are homogeneously distributed throughout the whole nanocomposite, but Co element is heterogeneously distributed. The Co and O signals are not overlaid with each other, that is to say, the nanoparticles with the size from 5 to 45 nm are not cobaltous oxide. Except the Co nanoparticles with the size from 5 to 45 nm, the part Co species was homogeneously distributed, which indicate that the Co species partly was stabilized by doping in the nanocomposite. The elemental analysis images (Figure 3g) further proved the presence of N, C, O, and Co components. High-resolution TEM (HRTEM, Figure 3h) revealed the existence of the Co nanoparticle, which indicates the resolved lattice fringe of the Co (111) plane with a spacing of 2.16 Å. Therefore, Co element exists in the nanocomposite in the forms of Co nanoparticles with the size from 5 to 45 nm and doping in the CMK3/G.

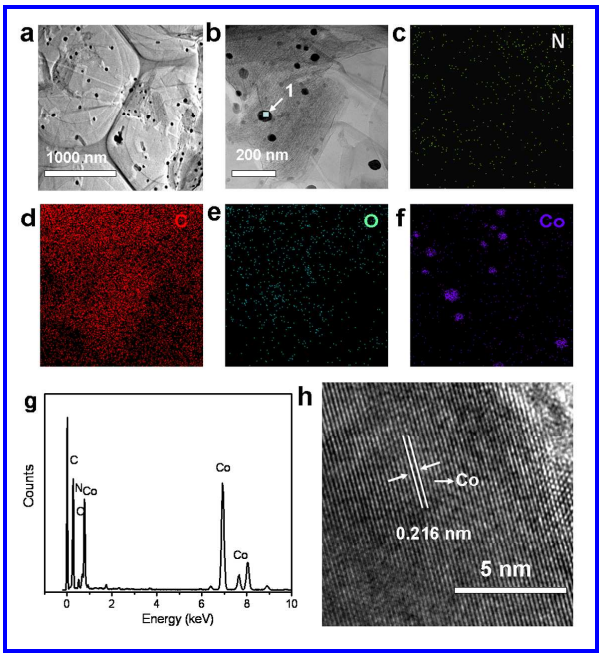


**Figure 3.** Characterizations of the typical CMK3/G-N-Co. (a-b) STEM images of the typical CMK3/G-N-Co; (c-f) nitrogen, carbon, oxygen and cobalt element mapping; (g) elemental analysis image of the typical CMK3/G-N-Co (square region marked with 1 in the Figure 1b); (h) HRTEM images of Co nanoparticles (square region marked with 1 in the Figure 1b)

X-ray diffraction was used to investigate the structure of the typical CMK3/G-N-Co. The XRD pattern (Figure 4a) confirmed the formation of Co (JCPDS no.15-0806) in the product. Three major reflections located at about 44.0°, 51.5° and 75.8° can be assigned to diffraction of Co with cubic-phase from the (111), (200) and (220) planes, respectively. Figure 4b shows the XPS survey of the typical CMK3/G-N-Co. The atomic percentage of C (88.95 at.%), O (3.37 at.%), N (6.98 at.%) and Co (0.69 at.%) can be reached, respectively. The high-resolution of N1s spectra of the typical product (Figure 4c) indicates that the pyridinic, pyrrolic, and graphitic-N were doped. The peak at 398.4 eV corresponds to pyridinic N species, the peak at 399.8 eV can be ascribed to

pyrrolic structure, and the peak at 401.1 eV belongs to graphitic N species. These results confirmed that the typical product was successfully doped by nitrogen element. Generally, pyridinic N and graphitic N are believed to participate in the active sites and improve the catalytical ability for ORR.[5,13,36] Figure 4d shows the nitrogen adsorption-desorption isotherm and Figure 4e shows pore size distribution of the CMK3/G-N-Co. The nanocomposite with mesoporous structure exhibits high BET surface area of 534.8 $m^2$ $g^{-1}$ and total pore volume of the 0.62 $cm^3$ $g^{-1}$. Raman spectra (Figure 4f) show that the typical product exhibits the remarkable peaks at around 1350 and 1585 $cm^{-1}$ corresponding to the well-defined D band and G band, respectively. In addition, a broader 2D peak appeared at around 2745 $cm^{-1}$, which is consistent with that of the other nitrogen-doped carbon material reported.[6,14]

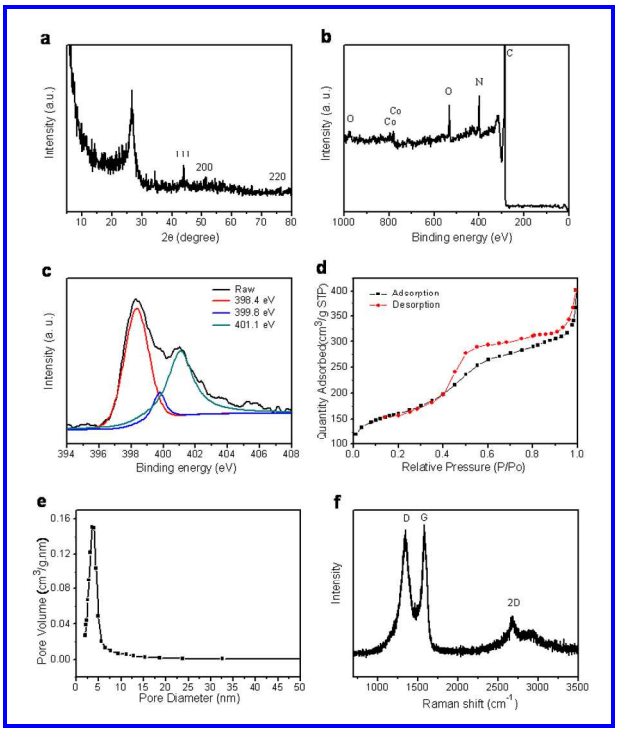


**Figure 4.** (a) XRD patterns; (b) XPS survey; (c) high-resolution N1s XPS spectra; (d) nitrogen adsorption-desorption isotherm；(e) pore-size distribution and (f) Raman spectra of the typical CMK3/G-N-Co nanocomposite.

### 3.3 The optimization of the experimental conditions

The effect of Co-content and annealing temperature and time on the performance of the catalyst was measured. In order to investigate the effect of Co content on the performance of the catalyst, we also prepared the CMK3/G-N-Co nanocomposite with Co content of 0.8 and 4.0 wt%, respectively. TEM images of the products were shown in the Figure S2a and b (see the Supporting Information). For comparison, the product based on CMK3, nitrogen, and trace cobalt (CMK3-N-Co), the product based on graphene, nitrogen, and trace cobalt (G-N-Co) and the product based on CMK3, graphene, nitrogen (CMK3/G-N) was synthesized, respectively. TEM images of the G-N-Co, CMK3-N-Co and CMK3/G-N were shown in the Figure S3 (see the Supporting Information). From the Figure 5a and b, it can be seen that the Co-content can obviously affect the half-peak potential and reduction current, and the catalyst shows best performance with Co content of 2.4 wt.%. We also researched the annealing temperature and time on the performance of the catalysts. The results were shown in the Figure 5c-f. The Figure 5c and d reveal the optimal annealing temperature is 950 $^oC$. From the Figure 5e and f, for the high half-peak potential and reduction current, the optimal annealing time was found to be 50 min. The effect of GO content in the preparation on the half-peak and reduction current were shown in the Figure 5g and h. In the preparation, when 60.0 mg CMK3 was used, the optimal GO content was found to be 30.0 mL (2.5 mg/ mL).

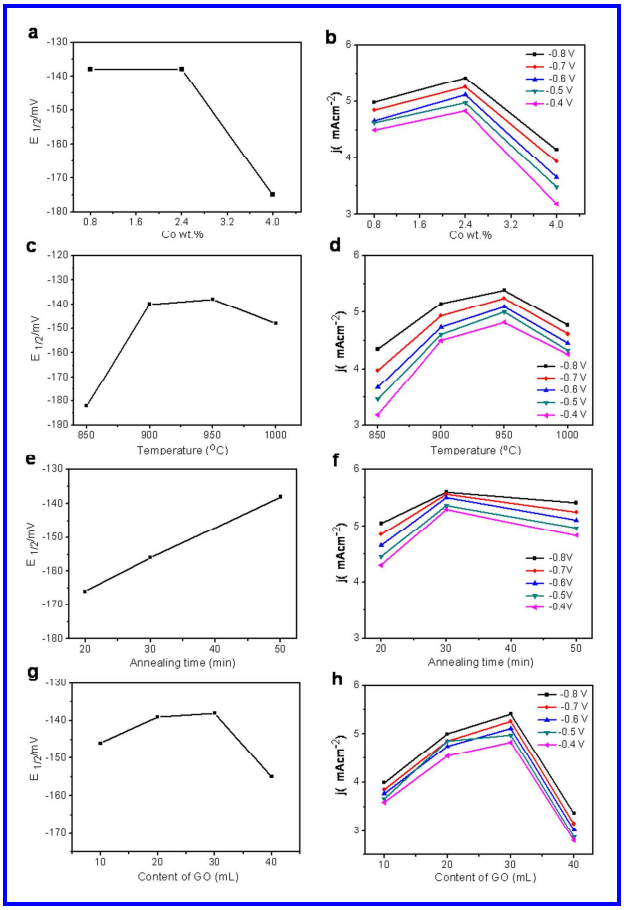


**Figure 5.** The optimization of the CMK3/G-N-Co. (a) The effect of Co-content on the half-peak; (b) The effect of Co-content on the reduction current; (c) The effect of annealing temperature on the half-peak; (d) The

effect of annealing temperature on the reduction current; (e) The effect of annealing time on the half-peak; (f) The effect of annealing time on the reduction current; (g) The effect of GO content on the half-peak and (h) The effect of GO content on the reduction current. The values of Co-content in the catalysts were obtained with ICP-MS.

In addition, an indirect way was used to test the role of the Co nanoparticles with the size from 5 to 45 nm in the product for the ORR. We prepared the CMK3/G-N-Co without the Co nanoparticles by treatment of the typical CMK3/G-N-Co using 0.5 M $H_2SO_4$ at 80°C for 10 h. Figure 6b shows the TEM images of the CMK3/G-N-Co without the Co nanoparticles. We compared the ORR activity of the typical CMK3/G-N-Co and the CMK3/G-N-Co without the Co nanoparticles (Figure 6a). Obviously, compared to the typical CMK3/G-N-Co, the CMK3/G-N-Co without the Co nanoparticles shows the low half-peak potential and reduction current. The half-peak potential is about 15 mV less than that of the typical CMK3/G-N-Co. Therefore, the Co nanoparticles with the size from 5 to 45 nm in the catalyst contribute to the high activity for ORR. We measured the percentage of cobalt element in the form of doping in the CMK3/G and in the form of nanoparticles. According to the percentage of cobalt element in the form of doping in the CMK3/G, the percentage of cobalt element in the form of nanoparticles was also obtained. The product P1-P6 was prepared when the 13.0 mg cobalt (II) acetate tetrahydrate was added, respectively. The results were shown in the Table S1 (see the Supporting Information). From the Table S1, the annealing temperature and time have obvious effects on the percentage of cobalt element in the form of doping in the CMK3/G and in the form of nanoparticles. According to the ORR property (Figure 1 and 5), we believe that the percentage of cobalt element in the form of doping in the CMK3/G and in the form of nanoparticles can affect the ORR property. In this study, in order to obtain the ideal ORR property, the optimal percentage of cobalt element in the form of doping and that in the form of nanoparticles is 11.6 % and 88.4 %, respectively.

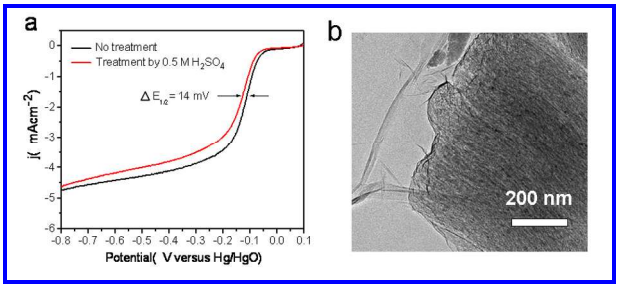


**Figure 6.** (a) RDE voltammograms in $O_2$-saturated 0.1 M KOH at room temperature for the typical CMK3/G-N-Co (No treatment) and the product treated by 0.5 M $H_2SO_4$; (b) TEM images of the Co-N-G/CMK without the Co nanoparticles by treatment of the Co-N-G/CMK using 0.5 M $H_2SO_4$ at 80°C for 10 h.

The ORR activities in the acidic media (0.5 M $H_2SO_4$) were also investigated by RDE measurements. The results were shown in the Figure 7. For the commercial Pt/C and CMK3/G-N-Co the value of onset potential was 650 and 505mV (vs Ag/AgCl), respectively (Figure 7a). The CMK3/G-N-Co shows good catalytic ability. Figure 7b shows the RDE voltammograms for the ORR on the CMK3/G-N-Co electrode at the rotation speed from 400 rpm to 2000 rpm. We tested the RDE voltammograms in $O_2$-saturated 0.5 M $H_2SO_4$ solution at room temperature for the CMK3/G-N-Co (Figure 7c) with or without methanol. The CMK3/G-N-Co shows excellent tolerance to methanol poisoning effects in 3.0 M $CH_3OH$. We also assessed the durability of the typical product in $O_2$-saturated 0.5 M $H_2SO_4$. Figure 7d shows that the typical product has a better durability than the Pt/C. According to the literatures reported, many of the non-precious metal or metal-free do not exhibit obvious activity for ORR in acidic media.[5, 37]

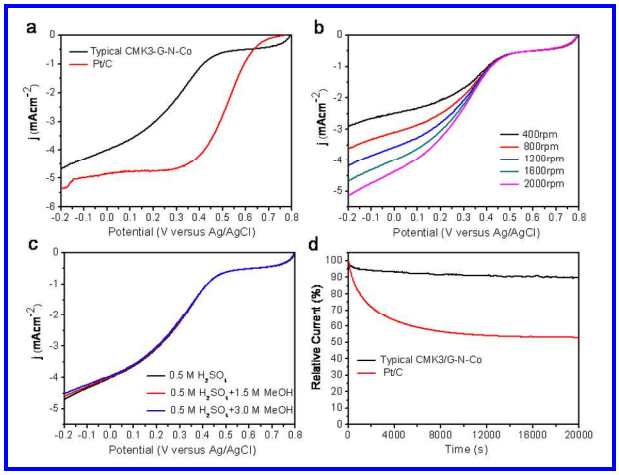


**Figure 7.** (a) RDE voltammograms in $O_2$-saturated 0.5 M $H_2SO_4$ at room temperature (rotation speed 1600 rpm, sweep rate 20 mV $s^{-1}$) for the CMK3/G-N-Co and Pt/C; (b) RDE voltammograms for the ORR at the CMK3/G-N-Co electrode at the various rotation speeds; (c) RDE voltammograms in $O_2$-saturated 0.5 M $H_2SO_4$ at room temperature (rotation speed 1600 rpm) for the CMK3/G-N-Co with or without methanol; (d) i-t chronoamperometric response of the CMK3/G-N-Co and Pt/C electrodes in $O_2$-saturated 0.5 M $H_2SO_4$ at a rotation rate of 800 rpm.

According to the above results, we believe that the excellent performance of the CMK3/G-N-Co is probably attributed to the

three reasons. First, the nitrogen and cobalt elements were doped in the CMK3/G to produce more active sites for ORR reaction.[18] Second, combining CMK3 with graphene will form a three-dimension nanoporous network structure, which effectively accelerates reactant, ion and electron transport.[11,28] Finally, the Co nanoparticles with the size from 5 to 45 nm in the catalyst contribute to the high activity for ORR. Because of the Co nanoparticles, the charge transfer across the carbon-Co interface and conductivity of the nanocomposite were promoted.[28,38]

## Conclusions

The electrocatalysts based on graphene, CMK3, nitrogen, and trace cobalt was prepared for the first time. The optimal CMK3/G-N-Co shows excellent catalytic ability, stability and tolerance to methanol poisoning effects in the alkaline media for ORR. The excellent performance is probably attributed to the doping of the nitrogen and cobalt elements in the CMK3/G, formation of a three-dimension nanoporous network structure by combining graphene with CMK3 and the promoted charge transfer across the carbon-Co interface and conductivity of the nanocomposite. So far, the graphene oxide and CMK3 have become the commercially available materials, therefore, the nanocomposite as electrocatalyst for ORR is the promising alternatives to Pt in fuel cells practical application. This research provides a new route to synthesize nonprecious-metal electrocatalyst by a low-cost, facile and readily scalable approach.

## Acknowledgements

We acknowledge the funding support from the National Natural Science Foundation of China (Grants 21271005, 91122025, 21471114), the State Major Research Plan (973) of China (No. 2011CB932404), Project of Science and Technology Head Introduction of Anhui University (02303203-0054) and the College Students' Innovation and Entrepreneurship Training Project (201310357137).

## Notes and references

[a] School of Chemistry and Chemical Engineering, Anhui University, Hefei, Anhui, 230601, P. R. China; E-mail: chenp123@ustc.edu.cn

[b] Department of Chemistry; Key Laboratory of Yangtze River Water Environment, Ministry of Education, Tongji University, Shanghai 200092, P. R. China; E-mail: qswu@tongji.edu.cn; Tel: 021-65982620, Fax: 086-021-65981097

Electronic supplementary information (ESI) available

[1] M. K. Debe, *Nature*, 2012, **486**, 43

[2] J. Suntivich, H. A. Gasteiger, N. Yabuuchi, H. Nakanishi, J. B. Goodenough, Y. Shao-Horn, *Nat. Chem*., 2011, **3**, 546

[3] R. Bashyam, P. Zelenay, *Nature*, 2006, **443**, 63

[4] D. S. Yu, E. Nagelli, F. Du, L. M. Dai, *J. Phys. Chem. Lett*., 2010, **1**, 2165

[5] Y. Zheng, Y. Jiao, M. Jaroniec, Y. Jin, S. Z. Qiao, *Small*, 2012, 3550

[6] P. Chen, T. Y. Xiao, H. H. Li, J. J. Yang, Z. Wang, H. B. Yao, S. H. Yu, *Acs Nano*, 2012, **6**, 712

[7] Y. Zheng, Y. Jiao, J. Chen, J. Liu, J. Liang, A. Du, W. M. Zhang, Z. H. Zhu, S. C. Smith, M. Jaroniec, G. Q. Lu, S. Z. Qiao, *J. Am. Chem. Soc*., 2011, **133**, 20116

[8] D. S. Geng, Y. Chen, Y. G. Chen, Y. L. Li, R. Y. Li, X. L. Sun, S. Y. Ye, S. Knights, *Energ. Environ. Sci*., 2011, **4,** 760

[9] Y. G. Li, W. Zhou, H. L. Wang, L. M. Xie, Y. Y. Liang, F. Wei, J. C. Idrobo, S. J. Pennycook, H. J. Dai, *Nat. Nanotechnol*., 2012, **7**, 394

[10] C. Z. Zhu, S. J. Dong, *Nanoscale*, 2013, **5**, 1753

[11] P. Chen, T. Y. Xiao, Y. H. Qian, S. S. Li, S. H. Yu, *Adv. Mater*., 2013, **25**, 3192

[12] K. P. Gong, F. Du, Z. H. Xia, M. Durstock, L. M. Dai, *Science,* 2009, **323**, 760

[13] L. T. Qu, Y. Liu, J. B. Baek, L. M. Dai, *Acs Nano,* 2010, **4**, 1321

[14] Z. H. Sheng, L. Shao, J. J. Chen, W. J. Bao, F. B. Wang, X. H. Xia, *Acs Nano*, 2011, **5**, 4350

[15] S. Chen, J. Y. Bi, Y. Zhao, L. J. Yang, C. Zhang, Y. W. Ma, Q. Wu, X. Z. Wang, Z. Hu, *Adv. Mater*., 2012, **24**, 5593

[16] L. S. Panchokarla, K. S. Subrahmanyam, S. K. Saha, A. Govindaraj, H. R. Krishnamurthy, U. V. Waghmare, C. N. R. Rao, *Adv. Mater*., 2009, **21**, 4726

[17] M. Lefevre, E. Proietti, F. Jaouen, J. P. Dodelet, *Science,* 2009, **324**, 71

[18] G. Wu, K. L. More, C. M. Johnston, P. Zelenay, *Science*, 2011, **332**, 443

[19] H. W. Liang, W. Wei, Z. S. Wu, X. L. Feng, K. Mullen, *J. Am. Chem. Soc*., 2013, **135**, 16002

[20] J. Liu, X. J. Sun, P. Song, Y. W. Zhang, W. Xing, W. L. Xu, *Adv. Mater*., 2013, **25**, 6879

[21] D. R. Dreyer, S. Park, C. W. Bielawski, R. S. Ruoff, *Chem. Soc. Rev*., 2010, **39**, 228

[22] S. Lee, S. H. Eom, J. S. Chung, S. H. Hur, *Chem. Eng. J*., 2013, **233**, 297

[23] K. H. Lee, B. Lee, S. J. Hwang, J. U. Lee, H. Cheong, O. S. Kwon, K. Shin, N. H. Hur, *Carbon*, 2014, **69**, 327

[24] J. Lee, J. Kim, T. Hyeon, *Adv. Mater*., 2006, **18**, 2073

[25] C. D. Liang, Z. J. Li, S. Dai, *Angew. Chem. Int. Edit*., 2008, **47**, 3696

[26] S. Jun, S. H. Joo, R. Ryoo, M. Kruk, M. Jaroniec, Z. Liu, T. Ohsuna, O. Terasaki, *J. Am. Chem. Soc*., 2000, **122**, 10712

[27] J. Wang, H. L. Xin, D. L. Wang, *Part. & Part. Syst. Char*., 2014, **31**, 515

[28] P. Chen, L.K. Wang, G. Wang, M.R. Gao, J. Ge, W.J. Yuan, Y.H. Shen, A.J. Xie, S.H. Yu, *Energ. Environ. Sci.*, 2014, **7**, 4095

[29] Z. Y. Wu, P. Chen, Q. S. Wu, L. F. Yang, Z. Pan, Q. Wang, *Nano Energy*, 2014, **8**, 118

[30] W. S. Hummers, R. E. Offeman, *J. Am. Chem. Soc*., 1958, **80**, 1339

[31] Y. Y. Liang, Y. G. Li, H. L. Wang, J. G. Zhou, J. Wang, T. Regier, H. J. Dai, *Nat. Mater*., 2011, **10**, 780

[32] M. K. Tham, R. D. Walker, K. E. Gubbins, *J. Phys. Chem*., 1970, **74**, 1747

[33] J. Liang, Y. Jiao, M. Jaroniec, S. Z. Qiao, *Angew. Chem. Int. Edit*., 2012, **51**, 11496

[34] J. Y. Choi, D. Higgins, Z. W. Chen, *J. Electrochem. Soc*., 2012, **159**, B87

[35] Y. Y. Liang, H. L. Wang, J. G. Zhou, Y. G. Li, J. Wang, T. Regier, H. J. Dai, *J. Am. Chem. Soc*., 2012, **134**, 3517

[36] H. Kim, K. Lee, S. I. Woo, Y. Jung, *Phys. Chem. Chem. Phys*., 2011, **13**, 17505

[37] D. W. Wang, D. S. Su *Energ. Environ. Sci.* 2014, **7**, 576.

[38] S. J. Guo, S. Zhang, L. H. Wu, S. H. Sun, *Angew. Chem. Int. Edit*., 2012, **51**, 11770

CMK3/G-N-Co catalytic system shows excellent catalytic ability in the alkaline media for oxygen reduction reaction and superior stability and tolerance to methanol poisoning effects compared to the Pt/C.